

ORIGINAL ARTICLE

The Influence of Anodizing Electrolyte Concentration on Ni-P Deposition on Anodic Aluminum Oxide (AAO)

Vika Rizkia^{1*}, Iwan Susanto², Belyamin¹, Vina Nanda Garjati¹, Ade Utami Hapsari³, Jarot Raharjo³, Damisih³, Retna Deca Pravitasari³

¹Department of Mechanical Engineering, Politeknik Negeri Jakarta, Jl Prof. Dr. G.A Siwabessy, Kampus Baru UI Depok, Depok City 16425, Indonesia

²Applied Master of Manufacturing Technology, Politeknik Negeri Jakarta, Jl Prof. Dr. G.A Siwabessy, Kampus Baru UI Depok, Depok City 16425, Indonesia

³Research Center for Advanced Materials, National Research and Innovation Agency (BRIN), 224 Building, Area Science and Technology B.J.Habibie, South Tangerang 15314, Indonesia

ABSTRACT – Aluminum alloys suffer from deficiencies in surface performance due to insufficient resistance to corrosion and mechanical qualities in harsh environments. Therefore, it is crucial to apply a protective surface modification during the manufacturing process of the aluminum component. The electroless deposited Ni-P shows great potential as a protective coating due to its simple manufacturing process and outstanding performance. This study investigates the effect of oxalic acid concentration in the anodizing process on electroless Ni-P coating. In this study, Anodic Aluminum Oxide (AAO) is formed by an anodizing process on 0.3, 0.5, and 0.7 oxalic acids prior to Ni-P electroless deposition. The resulting Ni-P layer has a nodular-like morphology with a size in the order of 0.5 μm or less. Moreover, the AAO surface is covered by a thin and tightly formed layer of nickel particles. The EDX analysis shows the oxygen percentage falls by up to 70% after Ni deposition in all anodizing parameters, as compared to the anodized specimens alone. In addition, the nickel content gradually decreases as the concentration of oxalic acid increases from 0.3 M to 0.7 M.

ARTICLE HISTORY

Received: 26 Feb 2025

Revised: 20 Apr 2025

Accepted: 30 May 2025

KEYWORDS

Electroless Deposition

Ni-P

Anodic Aluminum Oxide

Aluminum Alloy



Copyright © 2025 Author(s). Published by BRIN Publishing. This article is open access article distributed under the terms and conditions of the [Creative Commons Attribution-ShareAlike 4.0 International License \(CC BY-SA 4.0\)](https://creativecommons.org/licenses/by-sa/4.0/)

INTRODUCTION

Aluminum alloy is a lightweight, inexpensive, and readily accessible metal that is widely used in various industries. The extraordinary combination of low density and high ductility provides a promising future for aluminum products. It has significantly replaced mild steel, particularly in the automotive, aerospace, electronics, spacecraft, shipbuilding, medical, and other sectors[1], [2]. However, aluminum alloys exhibit shortages in surface performance as a result of inadequate corrosion resistance and mechanical properties in aggressive environments. Hence, it is essential to apply protective surface modification to the aluminum component production process[3], [4], [5].

Electroless deposition is a protective method that yields a uniform deposit characterized by low porosity and strong adhesion to the underlying surface. The process is simple, fast, and very low cost. Therefore, electroless coatings are frequently used as an aluminum surface modification method against corrosion attacks[6]. In particular, electroless Ni coatings have gained significant popularity due to their high hardness and exceptional resistance to wear, abrasion, and corrosion on aluminum alloys[7], [8]. According to earlier research, electroless nickel alloys can achieve high strength, improved tribo-mechanical properties, and corrosion resistance on an aluminum substrate[9], [10], [11], [12], [13], [14]. In addition, electroless nickel provides excellent uniformity in thickness and conformity to complex geometries, surpassing other protective coatings[15]. However, the tenacious and rapid oxide film formation on the aluminum surface decreases the adhesion between coatings and inner substrates. In this regard, prior to the deposition procedure on aluminum alloys, certain pretreatments are necessary.

Recently, the Anodic Aluminum Oxide (AAO) interlayer has gathered considerable interest in nanotechnology owing to its densely packed, self-assembled, and nanoscale porous structure. It is formed by anodizing in an acid electrolyte solution[16], [17], [18], [19]. The AAO provides strong adhesion as a result of the distinctive structure of the oxide interface and contributes significantly to the design of some ternary layers [20], [21]. Based on recent research[22], [23], [24], [25], a double-pretreatment procedure that involved anodic oxidation and surface activation phases was conducted on the aluminum alloy prior to the electroless Ni-P coating. The objective of the latter is to activate the surface for nickel deposition as well as to generate coatings with enhanced mechanical properties. The double pretreatment resulted in a highly effective electroless plating process and enhancements in the mechanical properties of the coating as well. Yazdi et al.[23] reported that the anodizing process generates a large number of

nanopores that facilitate mechanical interlocking and improve stress distribution. Moreover, it enhances adhesive bonding between electrocolored nickel and electroless Ni-P layer.

Regarding to creation of AAO structures with various dimensional sizes, the electrolyte solution used during the anodization process is one of the key factors determining the features of AAO. According to Erdogan et al.[26] raising the concentration of H_3PO_4 in the $\text{H}_3\text{PO}_4\text{-CrO}_3$ solution improves the regularity of AAO. In contrast, the addition of CrO_3 does not significantly affect the enhancement of AAO features. Giulia Scampone et al.[27] investigated the anodizing process on diecast $\text{AlSi}_{11}\text{Cu}_2(\text{Fe})$ alloy. The study demonstrated that a thicker AAO layer can be achieved by employing a combination of lower anodizing temperatures and a higher concentration of sulfuric acid. Moreover, Iwona Dobosz.[28] found that during the chemical treatment of oxide films in sulfuric and oxalic acid solutions, the pore diameter increases with the duration of pore widening, reaching a peak at approximately 120 min, after which the diameter remains constant. Conversely, in the case of the phosphoric acid solution, the pore diameter continues to increase throughout the observed time period.

A considerable amount of research on anodization indicates that the formation of pore morphology of AAO can be readily adjusted by altering anodization parameters. However, to the best of our knowledge, there is no scientific research that specifically addresses the effect of electrolyte solution concentration during the anodizing process on the deposition results of Ni-P on AA5052, a commercial AAO material.

EXPERIMENTAL METHOD

Materials

Aluminum AA5052 specimens, were purchased from Inti Logam Steel, were selected as the bare substrate for the Ni-P coating on AAO. The specimens were cut and then embedded in the epoxy resin with an exposed area of $1.5 \times 1.5 \text{ cm}^2$. The specimens were mechanically polished with successive grades of emery papers down to 1200 grit, washed with distilled water, degreased in 5% NaOH at 50°C for 3 min, and neutralized in 1:1 v:v HNO_3 at room temperature for 1 min. The specimens were then immediately washed with deionized water prior to anodic oxidation (anodizing).

Anodizing

Anodizing processes were conducted to produce AAO interlayers on the surface of aluminum 5052 specimens. A direct current power supply was used for the anodizing. The anodic oxidation process was conducted in a two-electrode beaker cell in 0.3, 0.5, and 0.7 M oxalic acid solution. Pure carbon and the specimens acted as the cathode and anode, respectively. The anodizing processes were conducted at room temperature under the voltage of 30 V for 3 h. After the anodic oxidation, the specimens were immersed in a solution of 5% phosphoric acid at 35°C for 10 min to further broaden the porous structure of the prepared AAO interlayer.

Ni-P Coating Process

The final step is the electroless deposition of Ni-P on the anodized specimens. As described by González-Gutiérrez et al.[29] the coating process was carried out in a solution containing 30 g.L^{-1} nickel sulfate as a source of Nickel, 20 g.L^{-1} sodium hypophosphite as a source of phosphorus and reducing agent, and 20 g.L^{-1} sodium citrate as a complexing ligand. The solution was maintained at 80°C and pH 5 for 60 min.

Microstructural Characterization

The surface morphology and elemental distribution of Ni-P coated AA5052 were examined using Field Emission Scanning Electron Microscopy FEI Inspect F50. It is equipped with an Energy Dispersive X-ray Spectroscopy (EDX) detector (Oxford Instruments X-MaxN 80). The FE-SEM was operated at an accelerating voltage of 15 kV.

RESULT AND DISCUSSION

Anodic Aluminum Oxide Morphology

The scanning electron micrograph of the AAO surface under anodizing electrolyte parameters of 0.3, 0.5, and 0.7 M oxalic acid with the constants voltage of 30 V, for 3 h at room temperature is shown in Fig. 1(a)-(c), respectively. It reveals the gradual growth and dissolution trend of AAO in 0.3, 0.5, and 0.7 M of oxalic acid solution. In Figure 1a, a compact arrangement of small nodes is observed, forming a nodular structure as a product of the anodizing process in 0.3M oxalic acid. In addition, the nodular structure creates a crater pattern with a clear edge and the tiny pores within the crater. The structure can be attributed to the migration of Al^{3+} ions from the metal through the interface between the metal and oxide and the development of the oxide layer. Meanwhile, O^{2-} ions migrate towards the oxide layer at the oxide/electrolyte interface[30].

The morphology of samples subjected to an anodizing process in 0.5 M oxalic acid is depicted in Figure 1b. The anodized specimens exhibited a distinct surface microstructure comprised of numerous nanopores. Evidently, the morphology of the nanopores in this specimen showed a regular formation characterized by an array of cylindrical nanopores. The geometry of each cylinder was structured in the shape of a hexagonal cell. This phenomenon due to the increase of oxalic acid concentrations enhance ionic mobility. Consequently, the system experiences greater availability of oxygen/hydroxide ions and accelerated release of aluminum ions from the substrate. These conditions favor faster oxide dissolution rates and the formation of pore structures[31]. Moreover, according to Nahavandi et al.[32] the

formation of hexagonal cells can be attributed to the equilibrium of surface tension forces. In this stage, the AAO growth seems to reach a threshold corresponding to a structure of hexagonal nanoporous.

In Figure 1c, as for the anodizing process in the electrolyte of 0.7M oxalic acid, pores were found to be arranged randomly and exhibited a lack of uniformity in both pore diameter and pore shape. The excessive increase of oxalic acid disrupts the growth-dissolution equilibrium. The structure transitioned from a nanoporous to a "mesh" design, representing a dissolution and merge of the pore with its adjacent pore. Moreover, the 0.7 M anodized specimen showed a thicker pore wall than that of the 0.5 M specimen. This phenomenon is related to the production of intense heat arising as the electrolyte concentration increases during the anodizing process, which leads to the dissolution and pore widening of AAO[33], [34].

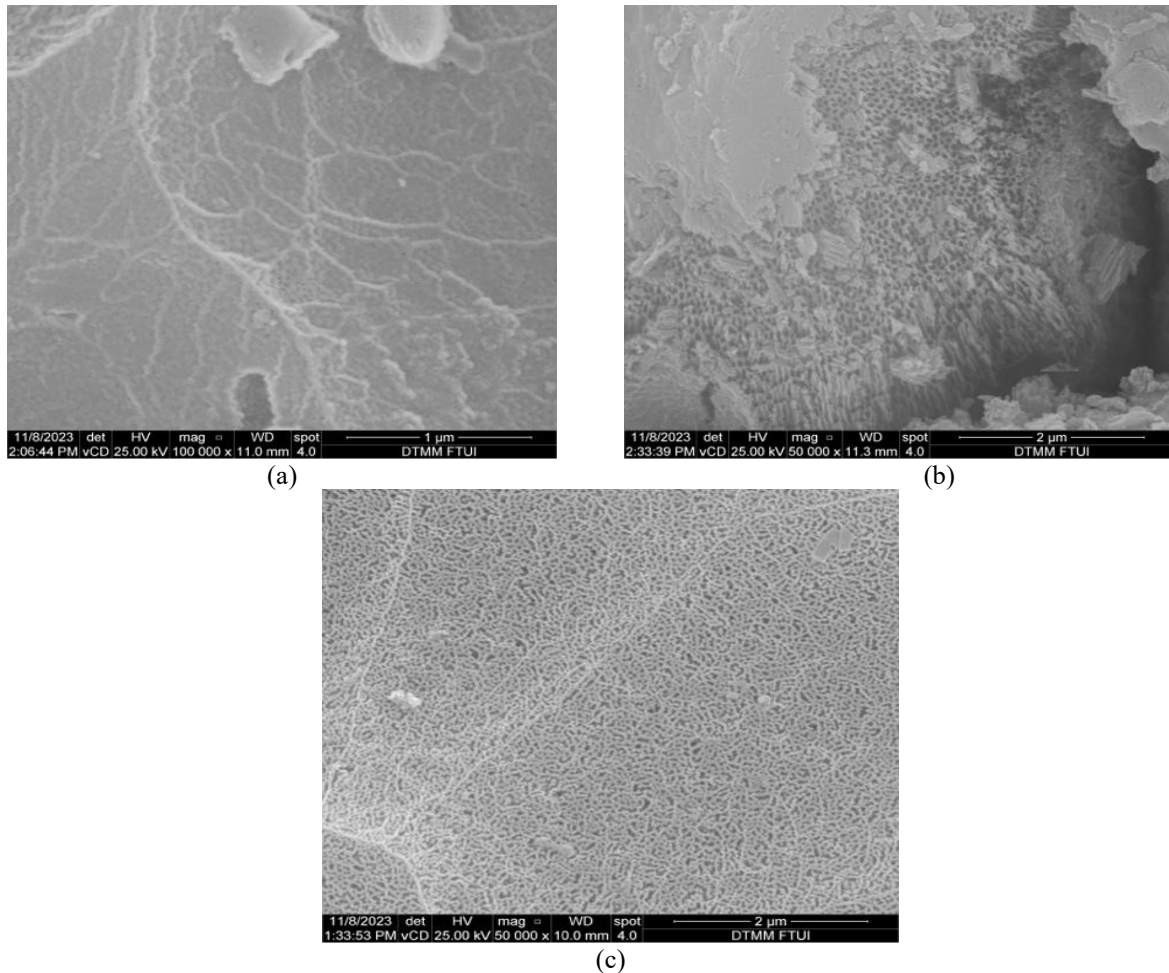


Figure 1. FE-FEM surface morphology of the AAO layer after the anodizing process in the electrolyte of a) 0.3 M, b) 0.5 M, and c) 0.7 M oxalic acid for 3 h at room temperature and the voltage of 30 V

In accordance with the chemical composition analyzed through EDX spectroscopy (Table 1), the anodized layer is predominantly composed of oxygen and aluminum in the Al_2O_3 stoichiometry.

Table 1. Weight and Atomic composition of the AAO layers grown by 3 h anodizing process at 30 V in various electrolytes, as deduced from EDX analysis

| | Al (wt%) | O (wt%) | Al (at%) | O (at%) |
|-------------------|----------|---------|----------|---------|
| 0.3 M Oxalic Acid | 53.69 | 46.31 | 40.74 | 59.26 |
| 0.5 M Oxalic Acid | 50.45 | 35.85 | 41.32 | 49.52 |
| 0.7 M Oxalic Acid | 55.36 | 44.64 | 42.38 | 57.62 |

Table 1 also indicates that there is a difference between concentrations of oxygen in the AAO layer produced by different anodizing parameters. The amount of oxygen content in the specimens conducted to the anodizing process of 0.3 M and 0.7 M oxalic acid remains the same. The AAO layer contains 46.31 wt% and 44.64 wt% of oxygen for 0.3 M and 0.7 M oxalic acid, respectively. The lowest oxygen percentage, about 35 wt%, was found in the AAO layer formed in the anodizing parameter of 0.5 M oxalic acid. This phenomenon accounts for the morphology of cylindrical nanopores in accordance with the FE-SEM image in Figure 1.

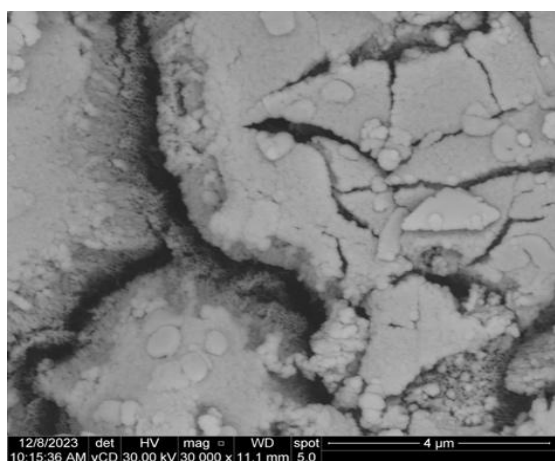
Ni Coating Morphology

In this study, the electroless Ni-P deposition was conducted directly on AAO interlayers without the existence of a surface activation agent.

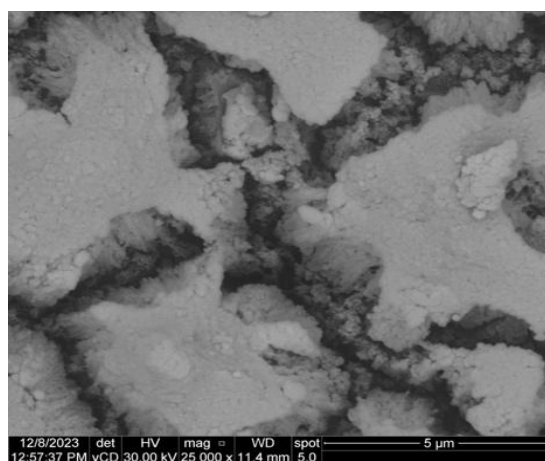
Fig. 2 illustrates the FE-SEM surface morphology of the coatings after Ni-P deposition on the anodized layer. The images clearly show the deposit of nickel nodules with a size in the order of 0.5 μm or less for all anodizing electrolytes studied. It could be observed that the AAO surface is covered by a thin and tightly formed layer of nickel. During the electroless deposition process, nickel ions infiltrate the pores of the anodized layer and initiate reduction there. The deposited nuclei then serve as catalytic sites for further nickel phosphorus deposition, as described by Backovic et al.[35]. Gutzeit [36] proposed that the nickel ion undergoes catalytic reduction through active atomic hydrogen, resulting in the simultaneous formation of orthophosphite and hydrogen ions. Moreover, Khan et al. [8] proposed that the catalytic dehydrogenation of adsorbed hypophosphite molecules on the surface leads to the release of atomic hydrogen, which subsequently reduces nickel at the catalyst surface. However, for all anodizing electrolytes studied, the electroless deposited Ni-P coatings directly applied to AAO exhibit inferior qualities including cracks. This phenomenon can be attributed to the failure of nickel cations to easily move through the pores of the anodized layer[1].

EDX analysis was carried out to investigate the coverage of Ni-P coating and to determine the composition of nickel and other elements during electroless nickel deposition onto AAO on the AA5052 surface at an immersion time of 60 min, room temperature, and pH 5 as shown in Table 2. As can be seen in Table 2, the percentage of oxygen after Ni deposition in all anodizing parameters decreases up to 70% compared to the amount of oxygen in Table 1. This phenomenon indicates that Ni deposits can cover the surface of AAO on the AA5052 substrate. Therefore, the oxygen accessibility to the AAO surface can be diminished by this layer. On the other hand, the increase in the percentage of aluminum (Al) can be attributed to the displacement of a portion of the surface oxide during the deposition process.

With respect to the nickel concentration in the coatings, the AAO retains the potential to serve as catalytic sites for nickel deposition, albeit with the formation of a thin Ni coating. Moreover, it could be observed that the nickel content slightly decreases with the increase in the concentration of oxalic acid from 0.3 M to 0.7 M. It can be associated with the surface morphology of AAO, as seen in Fig. 1. It is evident that the surface of AAO conducted from the anodizing process in 0.3 M oxalic acid is smoother than that of in the 0.5 and 0.7M oxalic acids. Therefore, the formation of nickel coating on this AAO interlayer is thicker. In brief, the presence of uniform and smooth surfaces of AAO interlayer provides more effective sites for the deposition of nanoparticles of nickel coatings.



(a)



(b)

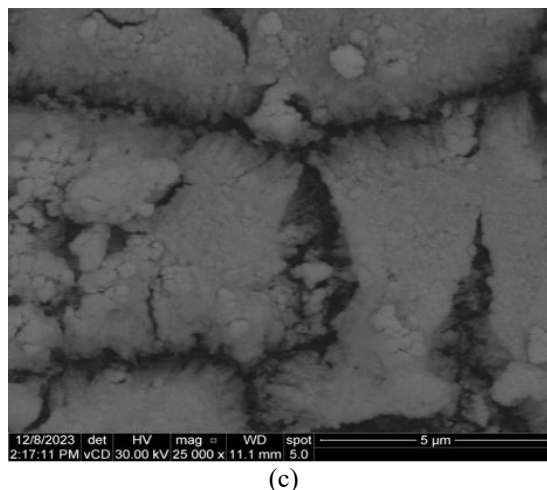


Figure 2. FE-FEM surface morphology of the AAO layer after the anodizing process in the electrolyte of a) 0.3 M, b) 0.5 M, and c) 0.7 M oxalic acid for 3 h at room temperature and the voltage of 30 V

Table 2. Weight and Atomic composition of the AAO layers grown by 3 h anodizing process at 30 V in various electrolytes, as deduced from EDX analysis

| | Al (wt%) | O (wt%) | Ni (wt%) |
|-------------|----------|---------|----------|
| 0.3 M + NiP | 72.49 | 13.70 | 08.27 |
| 0.5 M + NiP | 69.89 | 19.40 | 06.65 |
| 0.7 M + NiP | 78.18 | 15.95 | 05.87 |

CONCLUSION

In this study, in order to investigate the impact of electrolyte solution concentration during the anodizing process on the Ni-P; deposition results, the coating of Ni-P on Anodic Aluminum Oxide (AAO) was applied to the surface of aluminum AA5052 specimens with the absence of a surface activation agent. The AAO interlayer formed by an anodizing process in 0.3, 0.5, and 0.7 M oxalic acid. The primary conclusions are listed below:

- AAO produced by anodizing in 0.3M oxalic acid exhibited a crater-like structure with well-defined boundaries and small holes located within the craters. The 0.5 M oxalic acid anodized specimen displayed cylindrical nanopores that resembled hexagonal cells. Moreover, an anodized specimen of 0.7 M oxalic acid exhibited a structural transformation from a nanoporous to a "mesh" configuration.
- The results of Ni-P coating for all anodizing parameters indicate the formation of nickel nodules with a diameter of 0.5 μm or smaller on the AAO surface. Nevertheless, the electroless deposited Ni-P coatings that were applied directly to AAO demonstrated inferior qualities including cracks.

Moreover, the nickel content exhibits a gradual reduction when the concentration of oxalic acid increases from 0.3 M to 0.7 M. It was found that the best arrangement for Ni-P deposition on anodized AA5052 was obtained for an oxalic acid concentration of 0.3 M.

ACKNOWLEDGEMENT

The studies and analysis were performed with the financial support of the International Collaboration Research Grant, Politeknik Negeri Jakarta No. 385/PL3.A.10/PT.00.06/2024 on 25th April 2024.

REFERENCES

- [1] Y. Wang *et al.*, "Influence of pretreatments on physicochemical properties of Ni-P coatings electrodeposited on aluminum alloy," *Mater Des*, vol. 197, p. 109233, 2021.
- [2]. M. Abedini and S. Hanke, "Improving the wear resistance of aluminum by a nickel-filled anodized porous alumina layer," *Wear*, vol. 522, p. 204858, 2023.
- [3]. V. N. Kale, J. Rajesh, T. Maiyalagan, C. W. Lee, and R. M. Gnanamuthu, "Fabrication of Ni-Mg-Ag alloy electrodeposited material on the aluminium surface using anodizing technique and their enhanced corrosion resistance for engineering application," *Mater Chem Phys*, vol. 282, p. 125900, 2022.
- [4]. Z. Yin and F. Chen, "Effect of nickel immersion pretreatment on the corrosion performance of electroless deposited Ni-P alloys on aluminum," *Surf Coat Technol*, vol. 228, pp. 34–40, 2013.

- [5]. F. Davoodi, F. Ashrafizadeh, M. Atapour, E. Akbari-Kharaji, and R. Mokhtari, "Anticorrosion performance of TiN coating with electroless nickel-phosphorus interlayer on Al 6061 alloy," *Mater Chem Phys*, vol. 296, p. 127170, 2023.
- [6]. M. Sundararajan, M. Devarajan, and M. Jaafar, "Electroless NiB sealing on nanoporous anodic aluminum oxide pattern: deposition and evaluation of its characteristic properties," *Journal of Materials Research and Technology*, vol. 19, pp. 4504–4516, Jul. 2022.
- [7]. A. S. Kumar, K. Mohanam, G. Venkatachalam, S. Karthikeyan, and S. Narayanan, "Influence of Nickel Coating on Flexural and Dynamic Behaviour of Aluminium," *Procedia Eng*, vol. 97, pp. 1368–1378, 2014.
- [8]. E. Khan, C. F. Oduoza, and T. Pearson, "Surface characterization of zincated aluminium and selected alloys at the early stage of the autocatalytic electroless nickel immersion process," *J Appl Electrochem*, vol. 37, no. 11, pp. 1375–1381, 2007.
- [9]. P. Sahoo and S. K. Das, "Tribology of electroless nickel coatings – A review," *Mater Des*, vol. 32, no. 4, pp. 1760–1775, 2011.
- [10]. M. Gholizadeh-Gheslilagh, D. Seifzadeh, P. Shoghi, and A. Habibi-Yangjeh, "Electroless Ni-P/nano-WO₃ coating and its mechanical and corrosion protection properties," *J Alloys Compd*, vol. 769, pp. 149–160, 2018.
- [11]. J. P. Davim, S. Das, and P. Sahoo, "Roughness Optimization of Electroless Ni-B Coatings Using Taguchi Method," 2013, pp. 302–319.
- [12]. S. Kalyan Das and P. Sahoo, "Optimisation of tribological performance of electroless Ni–B coating using Taguchi method and grey relational analysis," *Tribology - Materials, Surfaces & Interfaces*, vol. 5, no. 1, pp. 16–24, Mar. 2011.
- [13]. S. Das and P. Sahoo, "Wear Performance Optimization of Electroless Ni-B Coating Using Taguchi Design of Experiments," *Tribology in Industry*, vol. 32, Dec. 2010.
- [14]. P. Sahoo and P. Gadhari, "Optimization of Friction and Wear Properties of Electroless Ni-P-Al₂O₃ Composite Coatings," *International Journal of Surface Engineering and Interdisciplinary Materials Science*, vol. 2, pp. 34–52, Jun. 2014.
- [15]. V. Vitry, J. Hastir, A. Mégret, S. Yazdani, M. Yunacti, and L. Bonin, "Recent advances in electroless nickel-boron coatings," *Surf Coat Technol*, vol. 429, p. 127937, 2022.
- [16]. D. Xu, H. Zhao, and C. Zhen, "Preparation of transparent anodic aluminum oxide films and their structural characteristics under thermal shock," *Microporous and Mesoporous Materials*, vol. 363, p. 112849, 2024.
- [17]. A. K. Eessaa and A. M. El-Shamy, "Review on fabrication, characterization, and applications of porous anodic aluminum oxide films with tunable pore sizes for emerging technologies," *Microelectron Eng*, vol. 279, p. 112061, 2023.
- [18]. L. Lerner, "Hard anodising of aerospace aluminium alloys," *Transactions of the Institute of Metal Finishing*, vol. 88, pp. 21–24, Jan. 2010.
- [19]. L. R. Krishna, Y. Madhavi, P. S. Babu, D. S. Rao, and G. Padmanabham, "Strategies for corrosion protection of non-ferrous metals and alloys through surface engineering," *Mater Today Proc*, vol. 15, pp. 145–154, 2019.
- [20]. T. I. Devyatkina, E. I. Yarovaya, V. V. Rogozhin, T. V. Markova, and M. G. Mikhaleenko, "Anodic oxidation of complex shaped items of aluminum and aluminum alloys with subsequent electrodeposition of copper coatings," *Russian Journal of Applied Chemistry*, vol. 87, no. 1, pp. 54–60, 2014.
- [21]. C. Zhou, Y. Wang, J. Chen, L. Xu, H. Huang, and J. Niu, "High-efficiency electrochemical degradation of antiviral drug abacavir using a penetration flux porous Ti/SnO₂-Sb anode," *Chemosphere*, vol. 225, pp. 304–310, 2019.
- [22]. M. Sundararajan, M. Devarajan, and M. Jaafar, "A novel sealing and high scratch resistant nanorod Ni-P coating on anodic aluminum oxide," *Mater Lett*, vol. 289, p. 129425, 2021.
- [23]. S. Shirmohammadi Yazdi, F. Ashrafizadeh, and A. Hakimizad, "Improving the grain structure and adhesion of Ni-P coating to 3004 aluminum substrate by nanostructured anodic film interlayer," *Surf Coat Technol*, vol. 232, pp. 561–566, 2013.
- [24]. J. Wang and Q. Wu, "The effects of anodic interlayer on the morphology and mechanical performances of electroless Ni–P coating on Al alloy," *Applied Physics A*, vol. 123, no. 6, p. 435, 2017.
- [25]. M. Kocabaş, C. Örnek, M. Curioni, and N. Cansever, "Nickel fluoride as a surface activation agent for electroless nickel coating of anodized AA1050 aluminum alloy," *Surf Coat Technol*, vol. 364, pp. 231–238, 2019.
- [26]. P. Erdogan, B. Yuksel, and Y. Birol, "Effect of chemical etching on the morphology of anodic aluminum oxides in the two-step anodization process," *Appl Surf Sci*, vol. 258, no. 10, pp. 4544–4550, 2012.
- [27]. G. Scampone, A. Russo, A. Carminati, and G. Timelli, "The influence of the electrolytic bath on the hard anodizing of diecast Al–Si–Cu alloys," *Results in Surfaces and Interfaces*, vol. 9, p. 100089, 2022.
- [28]. I. Dobosz, "Influence of the anodization conditions and chemical treatment on the formation of alumina membranes with defined pore diameters," *Journal of Porous Materials*, vol. 28, no. 4, pp. 1011–1022, 2021.
- [29]. A. Gutiérrez, M. Pech-Canul, and J. Sebastian, "Zincating Effect on Corrosion Resistance of Electroless Ni-P Coating on Aluminum Alloy 6061," *Fuel Cells*, vol. 17, pp. 770–777, Oct. 2017.
- [30]. Z. Wu et al., "Dual effects of ultrasound on fabrication of anodic aluminum oxide," *Ultrason Sonochem*, vol. 96, p. 106431, 2023.
- [31]. A. K. Eessaa and A. M. El-Shamy, "Review on fabrication, characterization, and applications of porous anodic aluminum oxide films with tunable pore sizes for emerging technologies," *Microelectron Eng*, vol. 279, p. 112061, 2023.
- [32]. M. Nahavandi and S. M. Monirvaghefi, "The effect of electroless bath pH on the surface properties of one-dimensional Ni–P nanomaterials," *Ceram Int*, vol. 46, no. 2, pp. 1916–1923, 2020.
- [33]. S. T. Abrahami, J. M. M. de Kok, V. C. Gudla, R. Ambat, H. Terryn, and J. M. C. Mol, "Interface strength and degradation of adhesively bonded porous aluminum oxides," *Npj Mater Degrad*, vol. 1, no. 1, p. 8, 2017.
- [34]. M. Noormohammadi, Z. S. Arani, A. Ramazani, M. A. Kashi, and S. Abbasimofrad, "Super-fast fabrication of self-ordered nanoporous anodic alumina membranes by ultra-hard anodization," *Electrochim Acta*, vol. 354, p. 136766, 2020.
- [35]. N. Backović, M. Jančić, and L. J. Radonjić, "Study of electroless Ni-P deposition on aluminium," *Thin Solid Films*, vol. 59, no. 1, pp. 1–12, 1979.
- [36]. G. Gutzeit, "Industrial Nickel Coating by Chemical Catalytic Reduction," *Transactions of the IMF*, vol. 33, no. 1, pp. 383–423, Jan. 1955.